Fracture studies of polycrystalline silicon based micro-electro-mechanical systems (MEMS)

Nanomechanics and nanotribology for reliability design of micro- and nano-systems - international exploratory workshop

24th October 2012

University of Liège
G. Becker, Shantanu S. Mulay, L. Noels

Université Catholique de Louvain
Renaud Vayrette, Jean-Pierre Raskin, Thomas Pardoen

Outline

- Introduction
- Numerical fracture framework for polycrystalline silicon
  - Discontinuous Galerkin (DG) method
  - Hybrid DG/Extrinsic cohesive law (ECL)
  - Orthotropic plane-stress Hooke's law for core of grains
  - Intra-granular fracture
  - Thickness effect
- Future work
  - Characterize inter-granular strength
  - Compare with experiments
  - Apply to robust design

Introduction

- Purpose
  - To develop a numerical method to predict MEMS fracture
- Difficulties
  - Grain sizes are no longer negligible compared to the structure size
  - Silicon is anisotropic
  - Inter/intra granular fractures
  - Dimensions are not perfectly controlled
  - Two MEMS will have
    - Different grains orientations/sizes
    - Different dimensions/surface profiles
- The numerical method should thus be probabilistic
  - But impossible to perform many direct numerical simulations with grain size resolutions

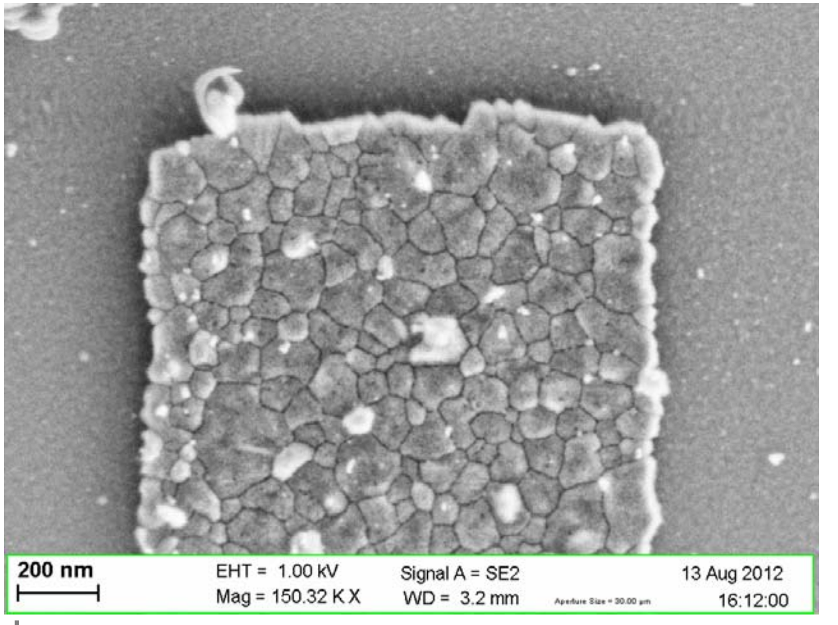

Introduction

- Objective is to develop a robust design procedure of MEMS based on numerical stochastic 3-scale approaches

Grain-scale Meso-scale MEMS scale

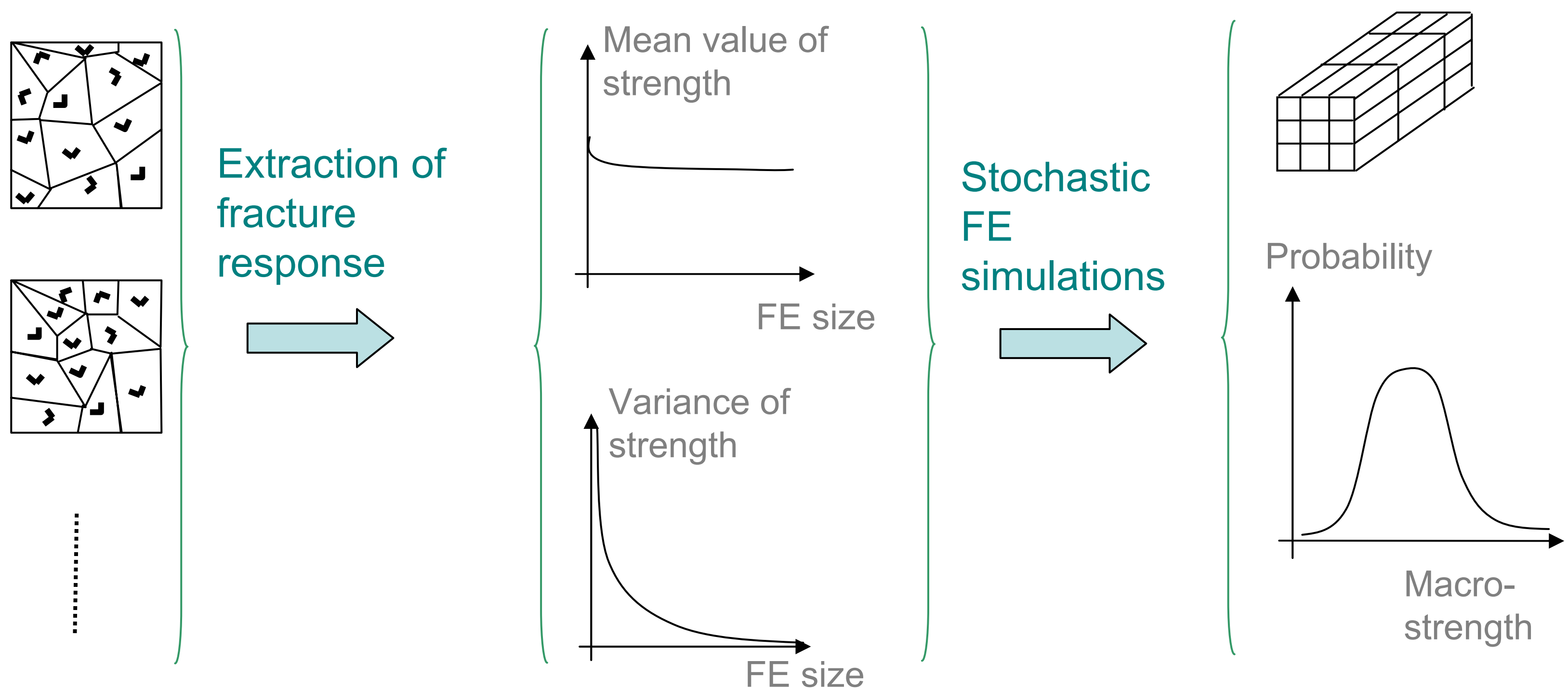

Introduction

- Methodology
  - Develop a numerical fracture framework for polycrystalline structures (ULg)
  - Validate tool with on-ship testing (UcL)

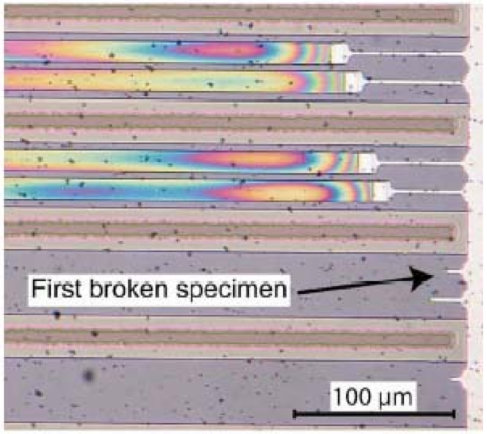

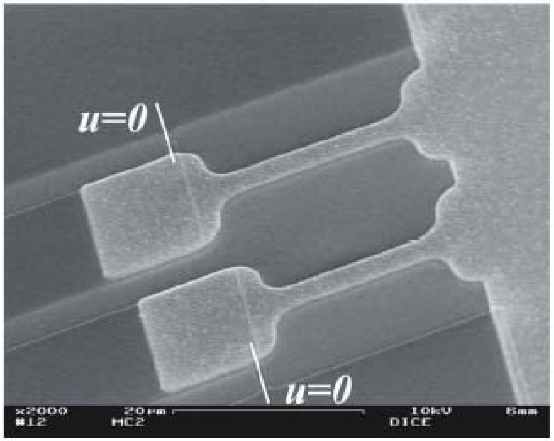

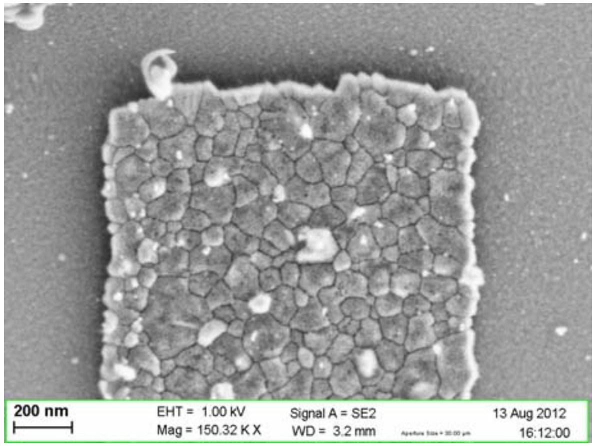

[Gravier et al., JMEMS 2009]

  - Exploit numerical fracture framework in the 3-scale stochastic method (future work)

Numerical fracture framework for polycrystalline silicon

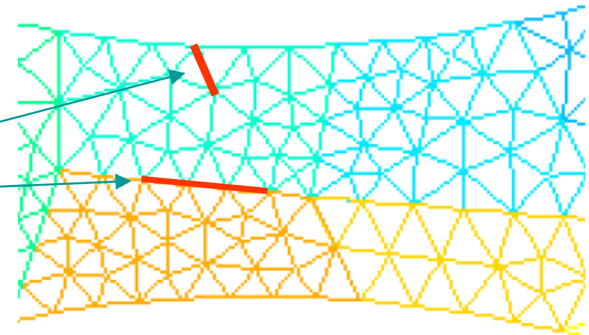

- Fracture challenges
  - Fracture can be
    - Inter-granular
    - Intra-granular
  - Grains are anisotropic
  - Initially there is no crack
- Numerical approach
  - Cohesive elements inserted between two bulk elements
  - They integrate the cohesive Traction Separation Law
  - Characterized by
    - Strength σ_c &
    - Critical energy release rate G_C
  - Can be tailored for
    - Intra/inter granular failure
    - Different orientations

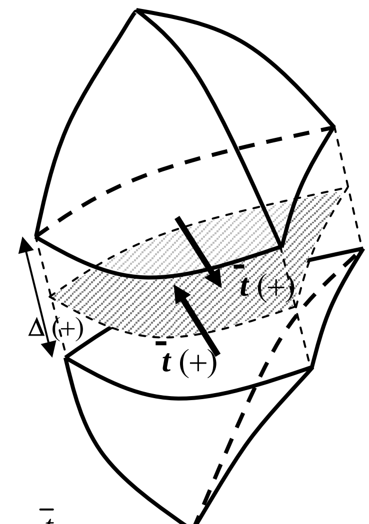

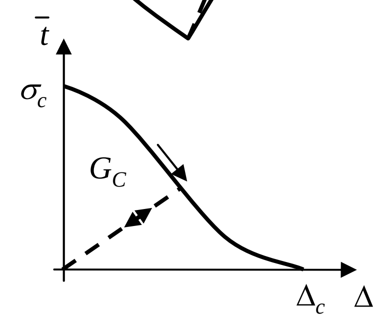

Numerical fracture framework for polycrystalline silicon

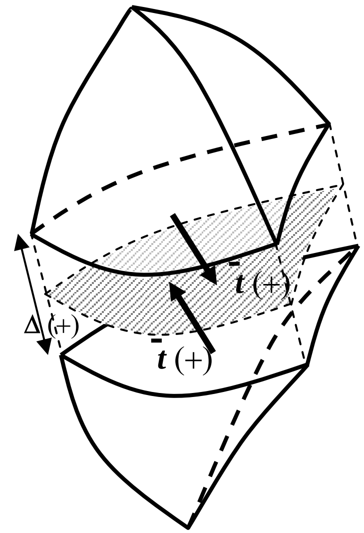

- Problems with cohesive elements
  - Intrinsic Cohesive Law (ICL)
    - Cohesive elements inserted from the beginning
    - Drawbacks:
      - Efficient if a priori knowledge of the crack path
      - Mesh dependency [Xu & Needelman, 1994]
      - Initial slope modifies the effective elastic modulus
      - This slope should tend to infinity [Klein et al. 2001]:
        - » Alteration of a wave propagation
        - » Critical time step is reduced

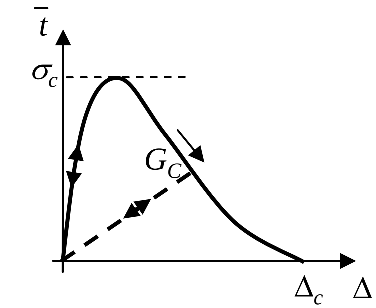

  - Extrinsic Cohesive Law (ECL)
    - Cohesive elements inserted on the fly when failure criterion is verified [Ortiz & Pandolfi 1999]
    - Drawback
      - Complex implementation in 3D (parallelization)

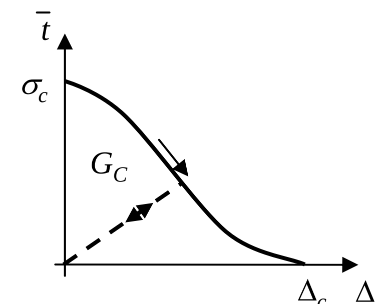

- Solution
  - Use discontinuous Galerkin methods embedding interface elements

Numerical fracture framework for polycrystalline silicon

- Discontinuous Galerkin (DG) methods
  - Finite-element discretization
  - Same **discontinuous** polynomial approximations for the
    - **Test** functions φ_h and
    - **Trial** functions $\delta\varphi$

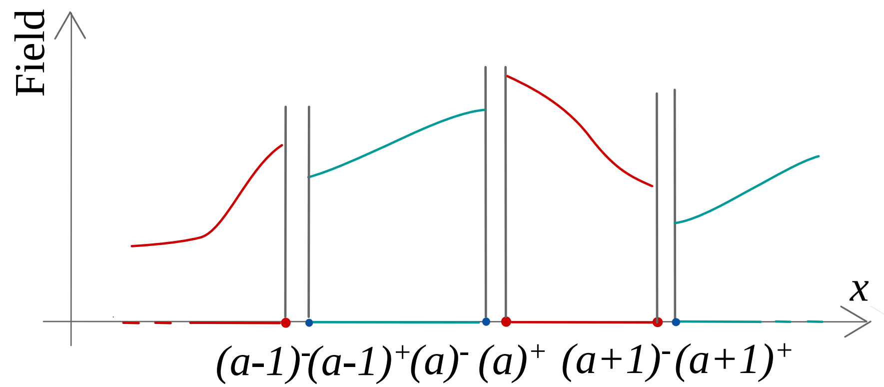

  - Definition of operators on the interface trace:
    - **Jump** operator: $[\![\bullet]\!] = \bullet^{+} - \bullet^{-}$
    - **Mean** operator: $\langle\bullet\rangle = \frac{\bullet^{+} + \bullet^{-}}{2}$
  - Continuity is weakly enforced, such that the method
    - Is consistent
    - Is stable
    - Has the optimal convergence rate

Numerical fracture framework for polycrystalline silicon

- Discontinuous Galerkin (DG) methods (2)
  - Formulation in terms of first Piola-Kirchhoff stress tensor $\mathbf{P}$

$$\boldsymbol{\nabla}_0 \cdot \mathbf{P}^T = 0 \text{ in } \Omega \quad \& \quad \begin{cases} \mathbf{P} \cdot \boldsymbol{N} = \bar{\boldsymbol{T}} \text{ on } \partial_N \Omega \\ \varphi_h = \bar{\varphi}_h \text{ on } \partial_D B \end{cases}$$

  - Weak formulation obtained by integration by parts **on each element** Ω^e

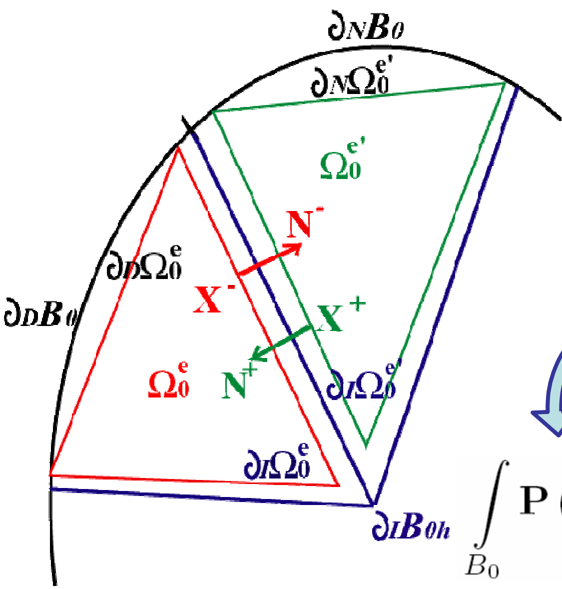

$$\sum_e \int_{\Omega_0^e} \boldsymbol{\nabla}_0 \cdot \mathbf{P}^T (\varphi_h) \cdot \delta\varphi \, dB = 0$$

$$\sum_e \int_{\Omega_0^e} -\mathbf{P}(\varphi_h) : \boldsymbol{\nabla}_0 \delta\varphi \, dB + \sum_e \int_{\partial\Omega_0^e} \delta\varphi \cdot \mathbf{P}(\varphi_h) \cdot \boldsymbol{N} \, d\partial B = 0$$

$$\int_{B_0} \mathbf{P}(\varphi_h) : \boldsymbol{\nabla}_0 \delta\varphi \, dB + \int_{\partial_I B_0} [\![\delta\varphi \cdot \mathbf{P}(\varphi_h)]\!] \cdot \boldsymbol{N}^- \, d\partial B = \int_{\partial_N B_0} \bar{\boldsymbol{T}} \cdot \delta\varphi \, d\partial B$$

New interface terms

- Discontinuous Galerkin (DG) methods (3)
  - Interface terms rewritten as the sum of 3 terms
  - Introduction of the numerical flux $\boldsymbol{h}$

$$\int_{\partial_I B_0} [\![\delta\varphi \cdot \mathbf{P}(\varphi_h)]\!] \cdot \boldsymbol{N}^- \, d\partial B \rightarrow \int_{\partial_I B_0} [\![\delta\varphi]\!] \cdot \boldsymbol{h}\left(\mathbf{P}^+, \mathbf{P}^-, \boldsymbol{N}^-\right) \, d\partial B$$

  - Has to be consistent: $\begin{cases} \boldsymbol{h}\left(\mathbf{P}^+, \mathbf{P}^-, \boldsymbol{N}^-\right) = -\boldsymbol{h}\left(\mathbf{P}^-, \mathbf{P}^+, \boldsymbol{N}^+\right) \\ \boldsymbol{h}\left(\mathbf{P}_{\text{exact}}, \mathbf{P}_{\text{exact}}, \boldsymbol{N}^-\right) = \mathbf{P}_{\text{exact}} \cdot \boldsymbol{N}^- \end{cases}$
  - One possible choice: $\boldsymbol{h}\left(\mathbf{P}^+, \mathbf{P}^-, \boldsymbol{N}^-\right) = \langle \mathbf{P} \rangle \cdot \boldsymbol{N}^-$

  - Weak enforcement of the compatibility

$$\int_{\partial_I B_0} [\![\varphi_h]\!] \cdot \left\langle \frac{\partial \mathbf{P}}{\partial \mathbf{F}} : \boldsymbol{\nabla}_0 \delta\varphi \right\rangle \cdot \boldsymbol{N}^- \, d\partial B$$

  - Stabilization controlled by parameter β, for all mesh sizes h^s

$$\int_{\partial_I B_0} [\![\varphi_h]\!] \otimes \boldsymbol{N}^- : \left\langle \frac{\beta}{h^s} \frac{\partial \mathbf{P}}{\partial \mathbf{F}} \right\rangle : [\![\delta\varphi]\!] \otimes \boldsymbol{N}^- \, d\partial B$$

  - Can also be explicitly derived from a variational form [Noels & Radovitzky, IJNME 2006 & JAM 2006]

Numerical fracture framework for polycrystalline silicon

- Hybrid DG/ECL
  - Interface terms exist at the beginning
    - DG method ensures consistency/stability
      [Seagraves, Jerusalem, Radovitzky, Noels, CMAME 2012]

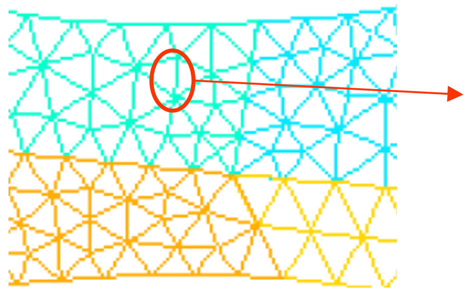

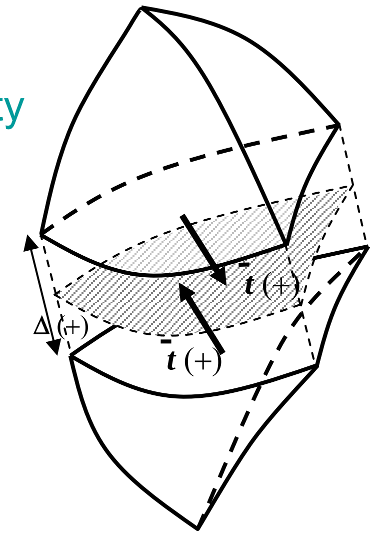

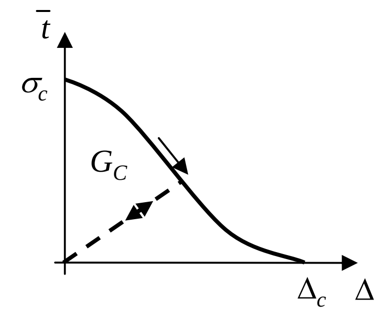

  - Onset of fracture
    - When interface traction reaches σ_c
    - The cohesive law substitutes for the DG terms
  - Advantages
    - Consistent
    - Easy to implement
    - Highly parallelizable
- In this work 2D plane-stress structures are studied

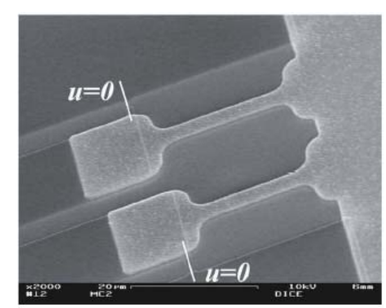

Numerical fracture framework for polycrystalline silicon

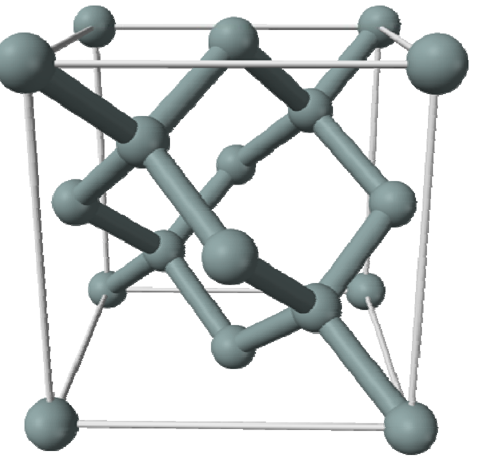

- Silicon crystal
  - Diamond-cubic crystal
  - Has symmetry-equivalent surfaces
  - Orthotropic material (at least two orthogonal planes of symmetry)
  - Different fracture strengths along crystal lattice planes
    - 6 {1 0 0}-directions, 12 {1 1 0}-directions, 8 {1 1 1}-directions

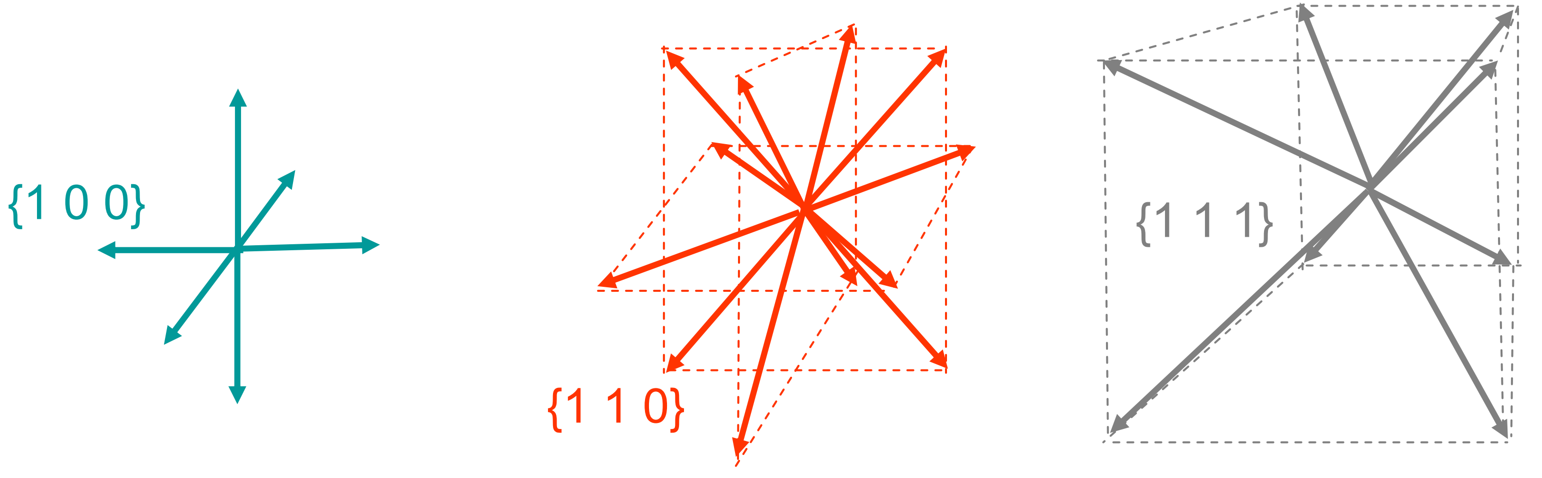

$$\sigma_{100} = 1.53\ \mathrm{GPa}, \sigma_{110} = 1.21\ \mathrm{GPa}, \sigma_{111} = 0.868\ \mathrm{GPa}$$

Numerical fracture framework for polycrystalline silicon

- Bulk law
  - In the referential (x, y, z) of the crystal
    - 9 constants (actually 3 ≠)

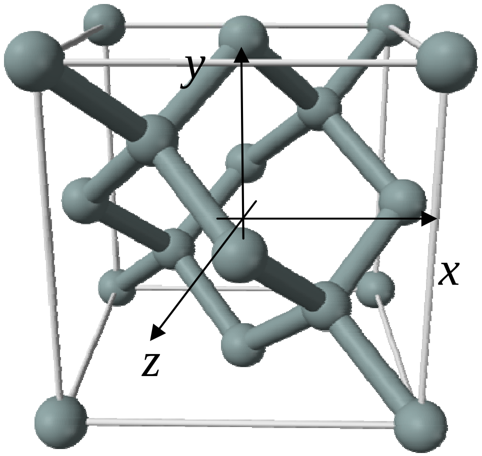

$$\begin{Bmatrix} \epsilon_{xx} \\ \epsilon_{yy} \\ \epsilon_{zz} \\ \epsilon_{xy} \\ \epsilon_{yz} \\ \epsilon_{zx} \end{Bmatrix} = \begin{bmatrix} \frac{1}{E_x} & \frac{-\nu_{yx}}{E_y} & \frac{-\nu_{zx}}{E_z} & 0 & 0 & 0 \\ \frac{-\nu_{xy}}{E_x} & \frac{1}{E_y} & \frac{-\nu_{zy}}{E_z} & 0 & 0 & 0 \\ \frac{-\nu_{xz}}{E_x} & \frac{-\nu_{yz}}{E_y} & \frac{1}{E_z} & 0 & 0 & 0 \\ 0 & 0 & 0 & \frac{1}{2G_{xy}} & 0 & 0 \\ 0 & 0 & 0 & 0 & \frac{1}{2G_{yz}} & 0 \\ 0 & 0 & 0 & 0 & 0 & \frac{1}{2G_{zx}} \end{bmatrix} \begin{Bmatrix} \sigma_{xx} \\ \sigma_{yy} \\ \sigma_{zz} \\ \sigma_{xy} \\ \sigma_{yz} \\ \sigma_{zx} \end{Bmatrix}$$

  - Is rotated in the referential axes (X, Y, Z)
    - Different angles for different grains
    - Plane stress state $\sigma_{ZZ} = 0$

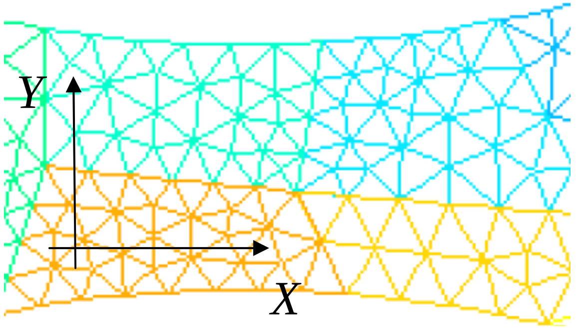

Numerical fracture framework for polycrystalline silicon

- Intra-granular fracture
  - Different fracture strengths along crystal lattice planes
    - 6 {1 0 0}-directions $\hat{\boldsymbol{n}}_1$, 12 {1 1 0}-directions $\hat{\boldsymbol{n}}_2$, 8 {1 1 1}-directions $\hat{\boldsymbol{n}}_3$
  - Mesh-interfaces are not along a fracture direction

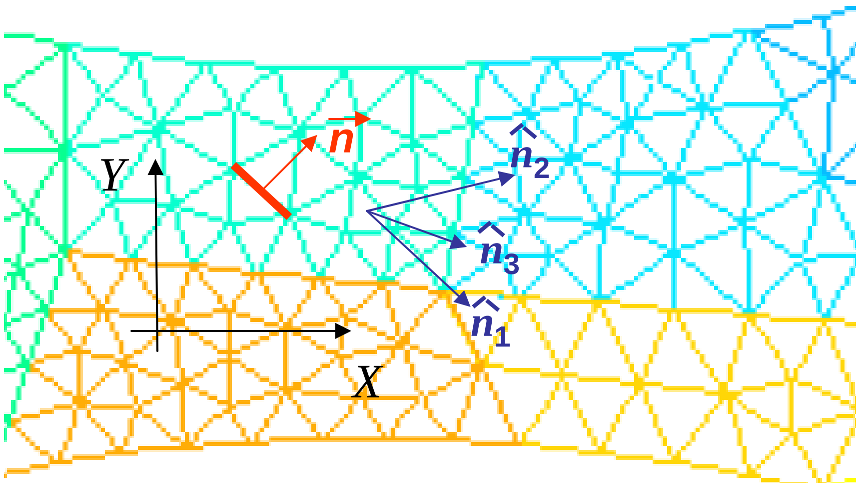

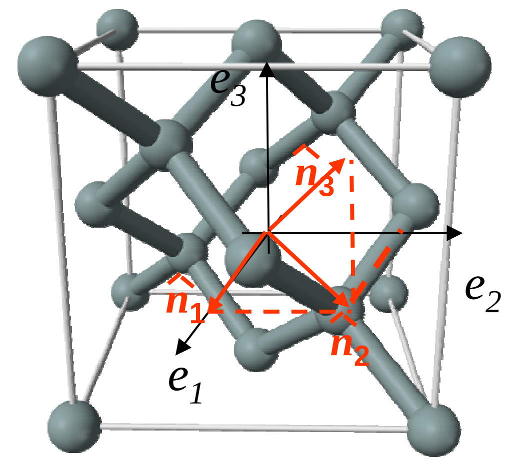

- Assumption: FE mesh > silicon crystal cell size (5.43 Å)
  - Compute effective fracture strength on any required plane
- But: $\hat{\boldsymbol{n}}_1$, $\hat{\boldsymbol{n}}_2$ & $\hat{\boldsymbol{n}}_3$ do not form an orthonormal basis
  - Consider the dual basis $\hat{\boldsymbol{n}}^1$, $\hat{\boldsymbol{n}}^2$ & $\hat{\boldsymbol{n}}^3$

Numerical fracture framework for polycrystalline silicon

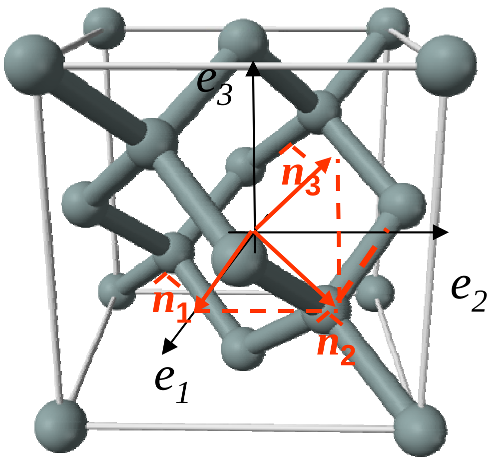

- Intra-granular fracture (2)
  - Surface normals of (1 0 0), (1 1 0), (1 1 1) known
    - $\hat{n}_1$, $\hat{n}_2$ & $\hat{n}_3$ do not form an orthonormal basis
    - Consider the dual basis $\hat{n}^1$, $\hat{n}^2$ & $\hat{n}^3$

$$\left.\begin{aligned} \hat{n}_1 &= \hat{e}_1 \\ \hat{n}_2 &= (1/\sqrt{2})(\hat{e}_1+\hat{e}_2) \\ \hat{n}_3 &= (1/\sqrt{3})(\hat{e}_1+\hat{e}_2+\hat{e}_3) \end{aligned}\right\} \Rightarrow \begin{aligned} \hat{n}^1 &= \hat{e}_1 - \hat{e}_2 \\ \hat{n}^2 &= \sqrt{2}(\hat{e}_2 - \hat{e}_3) \\ \hat{n}^3 &= \sqrt{3}\,\hat{e}_3 \end{aligned}$$

- Extract component of surface normal in the dual basis

$$\begin{cases} n^{100} = \vec{n}\cdot\hat{n}^1 \\ n^{110} = \vec{n}\cdot\hat{n}^2 \\ n^{111} = \vec{n}\cdot\hat{n}^3 \end{cases}$$

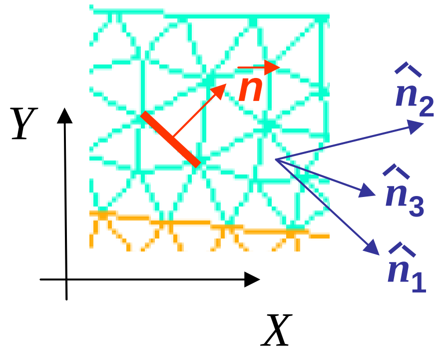

- Interpolate strength from strength along {1 0 0}, {1 1 0} and {1 1 1}

$$\vec{\sigma}_{eff} = \left[\sigma_{100}\, n^{100} + \frac{\sigma_{110}\, n^{110}}{\sqrt{2}} + \frac{\sigma_{111}\, n^{111}}{\sqrt{3}}\right]\hat{e}_1 + \left[\frac{\sigma_{110}\, n^{110}}{\sqrt{2}} + \frac{\sigma_{111}\, n^{111}}{\sqrt{3}}\right]\hat{e}_2 + \left[\frac{\sigma_{111}\, n^{111}}{\sqrt{3}}\right]\hat{e}_3$$

Numerical fracture framework for polycrystalline silicon

- Intra-granular fracture (3)
  - At the end of the day
    - $\sigma_{100} = 1.53\ \mathrm{GPa}, \sigma_{110} = 1.21\ \mathrm{GPa}, \sigma_{111} = 0.868\ \mathrm{GPa}$
    - $\|\vec{\sigma}_{eff}\| = \sqrt{\left(\sigma_{100}\, n^{100} + \frac{\sigma_{110}\, n^{110}}{\sqrt{2}} + \frac{\sigma_{111}\, n^{111}}{\sqrt{3}}\right)^2 + \left(\frac{\sigma_{110}\, n^{110}}{\sqrt{2}} + \frac{\sigma_{111}\, n^{111}}{\sqrt{3}}\right)^2 + \left(\frac{\sigma_{111}\, n^{111}}{\sqrt{3}}\right)^2}$
    - Applicable when surface normal is in-between the solid angle formed by $\hat{n}_1$, $\hat{n}_2$ & $\hat{n}_3$
    - 48 solid angles are identified in $\theta \in [0, 360]$ and $\phi \in [0, 180]$

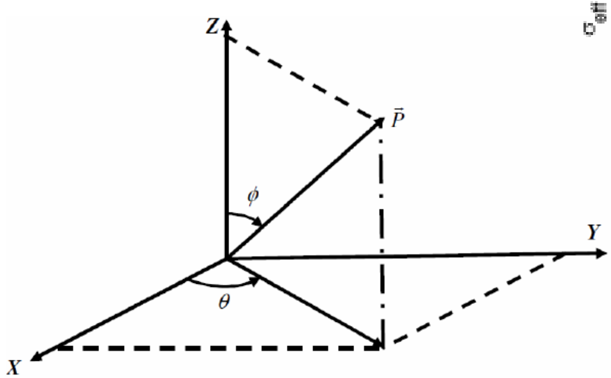

Spherical coordinate system

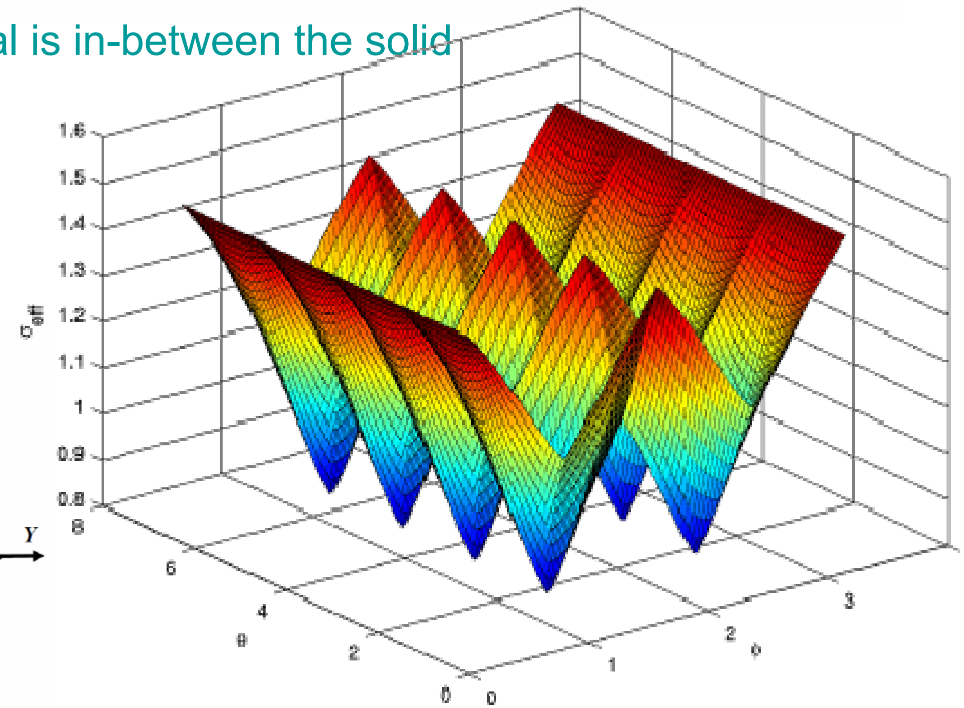

Numerical fracture framework for polycrystalline silicon

- Preliminary tests:
  - All the grains along the same direction
  - $\sigma_{100} = 1.53 \text{ GPa}, \sigma_{110} = 1.21 \text{ GPa}, \sigma_{111} = 0.868 \text{ GPa}$

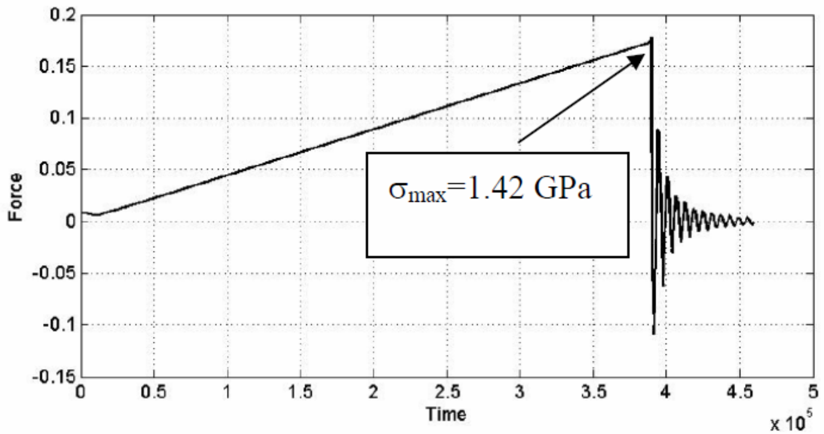

Fracture along {1 0 0}

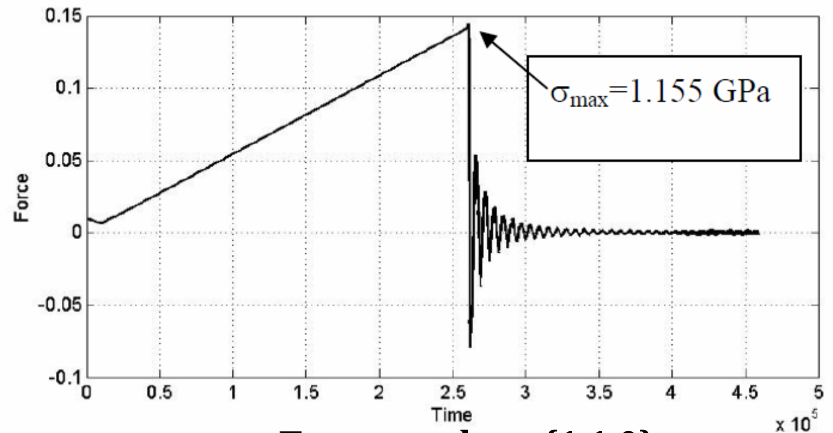

Fracture along {1 1 0}

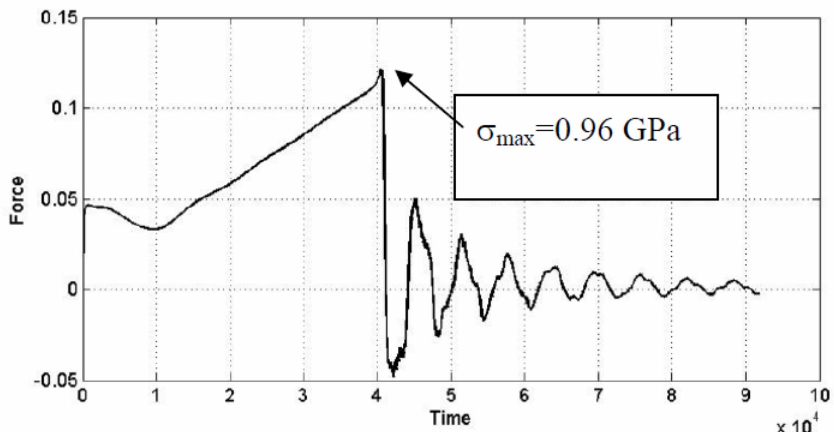

Fracture along plane {1 1 1}

Numerical fracture framework for polycrystalline silicon

- Thickness effect
  - 2D-plane-stress model
  - Reality is 3D
    - Anisotropy
    - Weakest plane is not always the section
  - Find weakest plane passing through the interface edge
    - Iterate on θ

$$\begin{Bmatrix} \hat{n}' \\ \hat{t}_0' \\ \hat{t}' \end{Bmatrix} = \begin{bmatrix} \cos(\theta) & \sin(\theta) & 0 \\ -\sin(\theta) & \cos(\theta) & 0 \\ 0 & 0 & 1 \end{bmatrix} \begin{Bmatrix} \hat{n} \\ \hat{t}_0 \\ \hat{t} \end{Bmatrix}$$

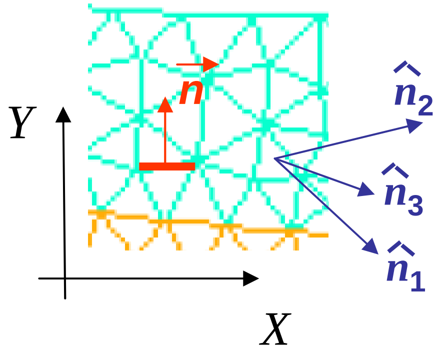

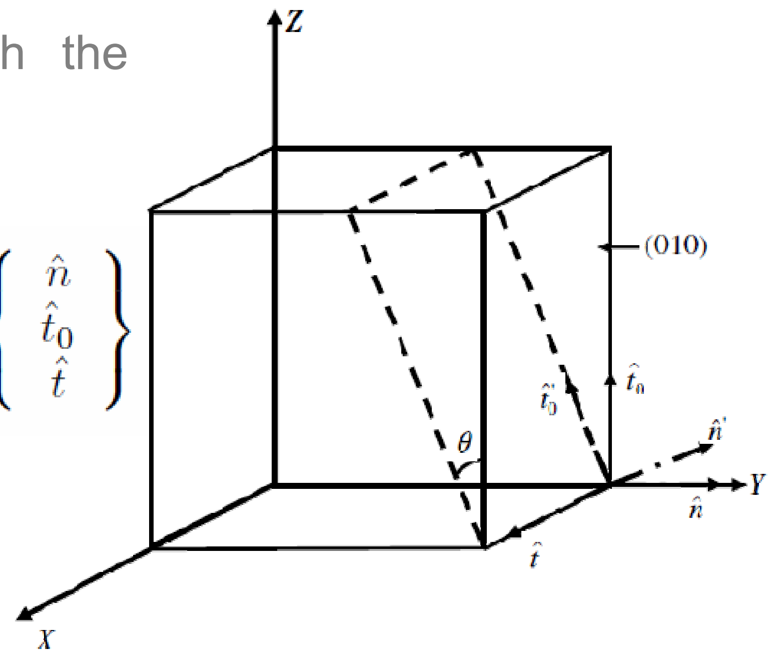

Rotation of interface element along thickness of MEMS

Numerical fracture framework for polycrystalline silicon

- Thickness effect (2)
  - Find weakest plane passing through the interface edge (2)
    - Iterate on θ
    - Compute new edge referential

$$\begin{Bmatrix} \hat{n}' \\ \tilde{t}_0 \\ \tilde{t} \end{Bmatrix} = \begin{bmatrix} \cos(\theta) & \sin(\theta) & 0 \\ -\sin(\theta) & \cos(\theta) & 0 \\ 0 & 0 & 1 \end{bmatrix} \begin{Bmatrix} \hat{n} \\ \hat{t}_0 \\ \hat{t} \end{Bmatrix}$$

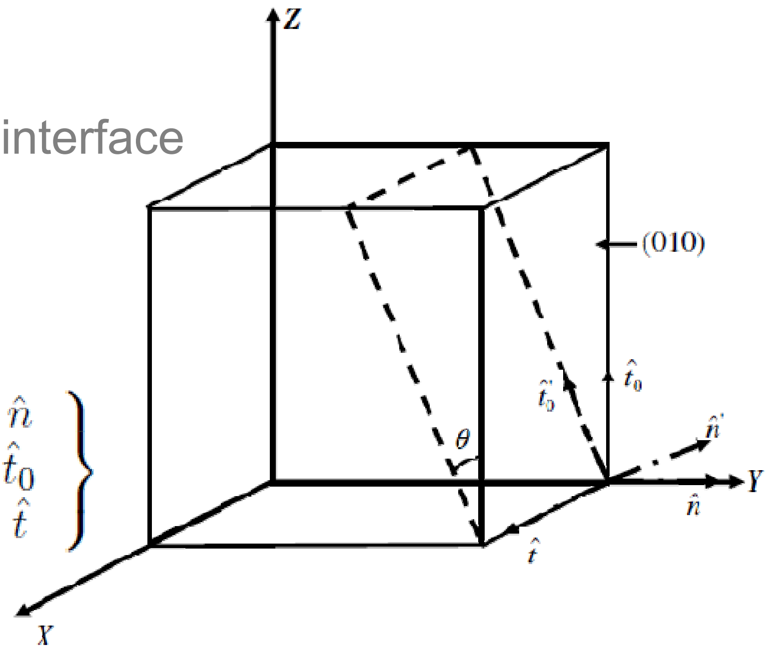

Rotation of interface element along thickness of MEMS

- Compute normal and tangential stresses in the new referential

$$\begin{cases} S_{nor} = (\sigma\,\hat{n}) \cdot \hat{n}' \\ \tau = (\sigma\,\hat{n}) \cdot \tilde{t} \\ \tau_0 = (\sigma\,\hat{n}) \cdot \tilde{t}_0 \end{cases} \Rightarrow \tau_{resultant} = \sqrt{(\tau)^2 + (\tau_0)^2}$$

- Compare these values to the strength along $\hat{n}'$
  - Extrapolated as previously

Future work

- Inter-granular strength
  - Characterize strength
  - In terms of mis-orientations
- Compare with experiments
  - Grains orientations by automated crystal oriented mapping (ACOM)
  - Analysis of the competition between inter-granular versus trans-granular crack path with respect to grain orientations

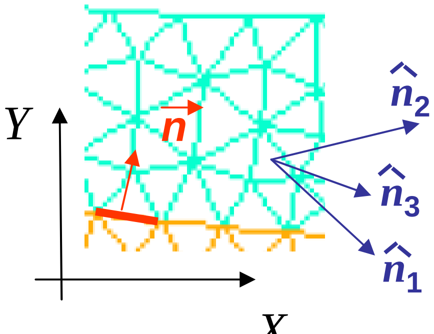

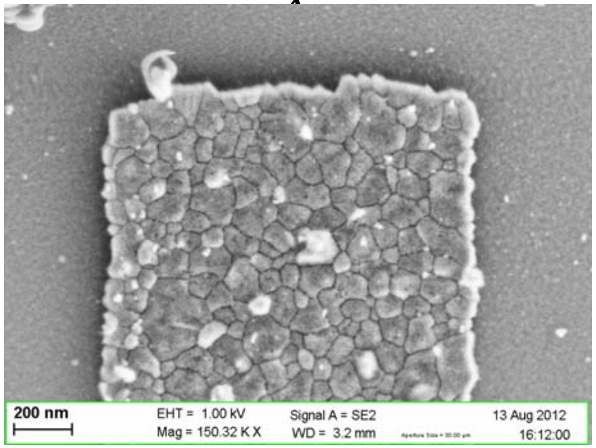

Future work

- Robust-design
  - Statistical fracture strength at meso-scale from micro-scale simulations involving different grain sizes and grain orientations
  - Stochastic numerical method considering statistical distribution of fracture strength

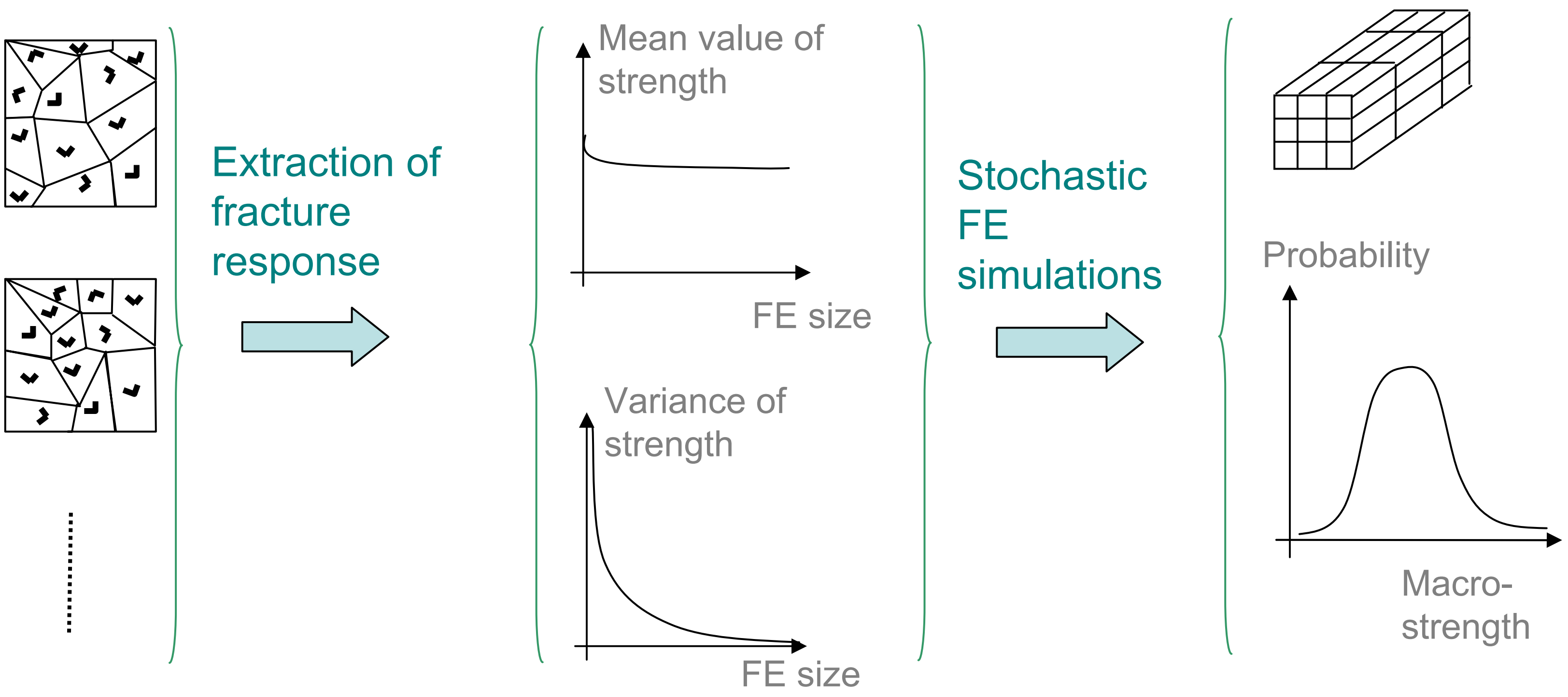

Thank you